

# Atmospheric aerosol deposition influences marine microbial communities in oligotrophic surface waters of the western Pacific Ocean

メタデータ	言語: eng 出版者: 公開日: 2017-12-05 キーワード (Ja): キーワード (En): 作成者: メールアドレス: 所属:
URL	<a href="http://hdl.handle.net/2297/46781">http://hdl.handle.net/2297/46781</a>

Title:

**Atmospheric aerosol deposition influences marine microbial communities in oligotrophic surface waters of the western Pacific Ocean**

Authors:

Teruya Maki\*<sup>1</sup>, Akira Ishikawa<sup>2</sup>, Tomoki Mastunaga<sup>1</sup>, Stephen B. Pointing<sup>3</sup>, Yuuki Saito<sup>1</sup>, Tomoaki Kasai<sup>2</sup>, Koichi Watanabe<sup>4</sup>, Kazuma Aoki<sup>5</sup>, Amane Horiuchi<sup>1</sup>, Kevin C. Lee<sup>5</sup>, Hiroshi Hasegawa<sup>1</sup>, Yasunobu Iwasaka<sup>6</sup>

Affiliation of all authors:

1. College of Science and Engineering, Kanazawa University, Kakuma, Kanazawa, Ishikawa 920-1192, Japan.
2. Graduate School of Bioresources, Mie University, 1577 Kurimamachiya, Tsu, Mie 514-8507, Japan.
3. School of Applied Sciences, Auckland University of Technology, 55 Wellesley Street East, Auckland 1010, New Zealand.
4. Department of Environmental Engineering, Faculty of Engineering, Toyama Prefectural University, 5180 Kurokawa, Imizu, Toyama 939-0398, Japan.
5. Department of Earth Sciences, Faculty of Science, University of Toyama 3190 Gofuku, Toyama 930-8555, Japan.
6. Community Research Service Group, University of Shiga Prefecture, 2500 Yasakamachi, Hikoneshi, Shiga, 522-8533, Japan.

\*Corresponding author:

Tel: +81-(0) 76-234-4793, Fax: +81-(0) 76-234-4800

E-mail: [makiteru@se.kanazawa-u.ac.jp](mailto:makiteru@se.kanazawa-u.ac.jp)

## Abstract

Atmospheric aerosols contain particulates that are deposited to oceanic surface waters. These can represent a major source of nutrients, trace metals, and organic compounds for the marine environment. The Japan Sea and the western Pacific Ocean are particularly affected by aerosols due to the transport of desert dust and industrially derived particulate matter with aerodynamic diameter less than 2.5  $\mu\text{m}$  (PM<sub>2.5</sub>) from continental Asia. We hypothesized that supplementing seawater with aerosol particulates would lead to measurable changes in surface water nutrient composition as well as shifts in the marine microbial community. Shipboard experiments in the Pacific Ocean involved the recovery of oligotrophic oceanic surface water and subsequent supplementation with aerosol particulates obtained from the nearby coastal mountains, to simulate marine particulate input in this region. Initial increases in nitrates due to the addition of aerosol particulates were followed by a decrease correlated with the increase in phytoplankton biomass, which was composed largely of Bacillariophyta (diatoms), including *Pseudo-nitzschia* and *Chaetoceros* species. This shift was accompanied by changes in the bacterial community, with apparent increases in the relative abundance of heterotrophic Rhodobacteraceae and Colwelliaceae in aerosol particulate treated seawater. Our findings provide empirical evidence revealing the impact of aerosol particulates on oceanic surface water microbiology by alleviating nitrogen limitation in the organisms.

Keywords: Asian dust; bacteria; oligotrophic ocean; phytoplankton; Aerosol deposition

## **1. Introduction**

Aerosols transported by westerly winds are a major source of nutrients, trace metals, and organic matter in the western Pacific Ocean (Jo et al., 2007) and Japan Sea (Tan et al., 2013). In oceanic areas where photosynthetic and heterotrophic microbial communities are nutrient-limited, aerosol deposition can supply both necessary trace elements and nutrients. The subsequent growth of primary producers affects marine productivity and carbon sequestration (Blank et al., 1985; Prospero and Savoie, 1989; Duce and Tindale, 1991; Spokes and Jickells, 1996; Erickson et al., 2003; Yuan and Zhang, 2006). Changes in the dynamics of bacterial communities induced by aerosol deposition to oceanic areas are also thought to vary the mineralization of organic matter and therefore affect marine carbon cycles (Lekunberri et al., 2010; Romero et al., 2011).

Recent economic and industrial development in continental Asia, particularly in China, has increased the emission of air pollution from the mainland coast (Chan and Yao, 2008). The deposition of anthropogenic aerosols from industrial regions delivers nutrients, such as nitrate and phosphate, to the ocean, significantly enhancing marine biological productivity along the Pacific Northwest coast (Zhang and Liu, 1994; Tan et al., 2011). Interestingly, trace elements, such as copper (Cu), found in dust particles have been reported to inhibit microbial growth in aquatic environments (Paytan et al., 2009; Jordi et al., 2012). Aerosol deposition inputs nutrients and trace elements to oligotrophic oceanic surface waters. The atmospheric input of nutrients into the North Pacific Ocean increases during short-term episodic deposition events during the high dust season (DiTullio and Laws, 1991). In the North Pacific Ocean, one large dust event

is found to have deposited aerosol particulates onto surface waters at a rate of approximately  $6.0 \text{ mg L}^{-1} \text{ one-event}^{-1}$  (Duce and Tindale, 1991). The annual deposition of dust generally varies between the Japanese coastal area ( $21 \text{ g m}^{-2}$ ) and the open ocean ( $0.8 \text{ g m}^{-2}$ ) (Uematsu et al., 2003). Deposited aerosols remain suspended within 40 m of the surface for up to 72 h (Hashimoto et al., 2005).

Dust events are also known to transport airborne microorganisms, supporting microbial recruitment to ecosystems downwind (Hervàs et al., 2009). Although previous studies have analyzed the influence of aerosols on marine ecosystems using model simulations and chemical analyses, there have been few incubation experiments that have directly assessed the response of marine microbial communities to aerosol deposition (Lekunberri et al., 2010; Romero et al., 2011). Incubation experiments using aerosol-treated seawater samples are affected by several constraints. Some studies have investigated microbial dynamics in marine and lake water samples treated with dust particulates and incubated under laboratory conditions (Paytan et al., 2009; Lekunberri et al., 2010). However, the time required for the transfer of open ocean seawater samples to the laboratory affects the microbial community. Shipboard incubation experiments can overcome this issue. Another challenge consists of collecting the large volumes of aerosols required to perform seawater incubation experiments.

During the winter and early spring, strong northwesterly winds result in heavy snowfall on Mt. Tateyama (3,015 m above sea level), which faces the Japan Sea. Aerosols are transported in a predictable manner by westerly wind from continental Asia to Japan and are preserved in the snowfall without undergoing local contamination

(Osada et al., 2004; Watanabe et al., 2011). Snow cover is therefore regarded as a product of continuous precipitation during the Asian dust season, and can be a useful source of aerosol particulates.

Here, we report a shipboard experiment undertaken in the Pacific Ocean to assess the impact of aerosol particulates, at levels typically experienced by oceanic surface waters on marine microbial communities. We used a combination of physicochemical analyses, direct cell counting and high-throughput sequencing approaches to identify changes in phytoplankton and heterotrophic microbial communities.

## **2. Materials and Methods**

### **2.1. Aerosol particulate recovery**

To prepare aerosol samples for shipboard experiments, snow samples containing aerosol particulates (dust particles and PM<sub>2.5</sub> pollution particles) were collected from snow cover at Murododaira on Mt. Tateyama (36.57°N, 137.60°E; 2,450 m, MR; Fig. 1) on 21 March 2012. At this location, strong northwesterly winds result in heavy snowfall during the winter and early spring leading to the deposition of aerosol particulates originating from the Asian continent (Watanabe et al., 2011). After a snow pit was dug, the walls of the pit were carefully smoothed to ensure the stratigraphy of the snow layer was undisturbed. The snow layers were composed of compacted or solid-type snow and included layers of melted and refrozen water (ice). In particular, the layer from the snow surface to a depth of 150 cm were included in the brown-color layers (dirty layers) that had not melted. Therefore, these snow layers would be expected to essentially maintain

the record of atmospheric aerosol deposition, revealing chemical compound dynamics from the top of the snow wall to a depth of 615 cm (Fig. S1). The snow layer at a depth of 110 cm was a non-white color (to be referred to as the “dirty” layer) and had higher concentrations of mineral particles ( $1.90 \times 10^5$  particles mL<sup>-1</sup>) and calcium (18.8  $\mu\text{eq L}^{-1}$ ) than other snow layers. The dirty layer harbored Na<sup>+</sup> at a concentration of 13.8  $\mu\text{eq L}^{-1}$ , which primarily originated from sea salt. The contribution of sea salt Ca<sup>2+</sup> to the total Ca<sup>2+</sup> content was minor (approximately 3%). The solutions of snow samples from a depth of 110 cm contained nss-Ca<sup>2+</sup> at a high concentration of 18.2  $\mu\text{eq L}^{-1}$ , suggesting that the mineral particles in the snow layers specifically contained calcium, which is a trace mineral found in Asian-dust mineral particles (Suzuki and Tsunogai, 1993). Snow was recovered aseptically from a subsurface of a dirty snow layer at a depth of 110 cm. We extrapolated LIDAR measurements of dust events and used back-trajectory analysis to establish the origin of this dust, deposited from the 1st to the 3rd of April 2012, in mainland Asia (Fig. S2). The snow samples were stored in polycarbonate bottles that were washed in a 3 mol L<sup>-1</sup> HCl solution and sterilized at 121°C for 20 min to remove metal, nitrate, and phosphate contamination, and frozen at -80°C until further analysis.

## **2.2. Seawater incubations**

Seawater sampling and shipboard experiments were performed 70 km off the coast of Omaezaki in the Shizuoka prefecture (34.07°N, 138.77°E) on 26 May 2012 during the SE526 cruise of T/S Seisui Maru (Mie University) (Fig. 1). At this sampling site, the

water column is thermally stratified from spring through summer, and the seawater temperature during the sampling periods decreased from 19.2 °C to 18.7 °C between a depth of 10 m and 18 m, indicating the presence of a weak thermocline (Fig. S3). These results suggest that the sampling area was oligotrophic on 26 May 2012. The nutrients in the surface layers are consumed by microbial activity, often causing oligotrophic conditions in the surface of the Pacific Ocean around Japan (Hashimoto et al., 2005). Seawater samples were collected from the surface at a depth of less than 1 m and stored in 20-L and 4-L sterilized holding tanks. One 20-L and two 4-L experimental tanks were used for each treatment, including ones filled with water as the control (C), ones with water exposed to 0.05 mg L<sup>-1</sup> of aerosols simulating a light dust event (LS), and with water exposed to 0.25 mg L<sup>-1</sup> of aerosols simulating a heavy dust event (HS). Treatments were incubated onboard the ship at surface temperature (24°C) under ambient light conditions for a 72-h period. Initial measurements were conducted 30 minutes after addition of aerosol particulates, with 24-h sample intervals thereafter.

### **2.3. Water chemistry**

For seawater samples, nitrate concentration was determined colorimetrically (Strickland and Parsons, 1972) after first removing particulates by filtration through 0.2 µm pore-size polycarbonate filters (Millipore, Tokyo, Japan). Inorganic phosphorus, as well as particulate and dissolved organic phosphorus, were measured using the molybdenum blue method (Strickland and Parsons, 1972). Iron in seawater samples was measured using ICP-AES.

## **2.4. Particulate estimates**

Water samples were fixed with a paraformaldehyde solution at a final concentration of 1%, stained with DAPI (4', 6-diamidino-2-phenylindole), and processed through a 0.22  $\mu\text{m}$  pore-size polycarbonate filter (Whatman, Tokyo, Japan; Russell et al., 1974). Cells and particulates on the filter were observed using an epifluorescence microscope (Olympus, Tokyo, Japan). Bacterial particles and yellow particles observed on the filter transect were counted. The detection limit of each particle was  $10^4$  particles  $\text{mL}^{-1}$  seawater, and  $10^3$  particles per filter. Yellow particles stained with DAPI were classified as organic matter (Mostajir et al., 1995). The majority of the yellow particles were not found in the snow sample solutions after protease treatment, suggesting that they were composed of proteins (Fig. S4). In seawater, phytoplankton and cyanobacteria can be observed using the DAPI staining technique, but we rarely counted these cells, as they were broken by the paraformaldehyde fixation and the filtration processes. Accordingly, we used this technique for counting bacterial and yellow particles only.

## **2.5. Phytoplankton biomass estimation and identification**

Phytoplankton biomass was estimated using Chl *a* concentration of 4 size fractions in the 20 L experimental tanks. A 200 mL aliquot of each sample was gravity filtered through a 20- $\mu\text{m}$  mesh (>20  $\mu\text{m}$  fraction). The filtrate was sequentially gravity filtered through Nuclepore filters (ADVANTEC, Tokyo, Japan) with a pore size of 10  $\mu\text{m}$

(10–20  $\mu\text{m}$  fraction), then passed through a 2- $\mu\text{m}$  filter (2–10  $\mu\text{m}$  fraction) with a vacuum pressure of <50 mmHg, and finally through a Whatman GF/F glass fiber filter (ADVANTEC, Tokyo, Japan) (<2  $\mu\text{m}$  fraction) with a vacuum pressure <100 mmHg. The Chl *a* retained on the filters was extracted in N,N-dimethylformamide at -20°C for 24 h (Suzuki and Ishimaru, 1990), and its concentration was determined using the fluorometric method defined previously by Parsons et al. (1984) with a Turner Design fluorometer Model 10-AU-005 (Turner Designs, CA, USA).

Microscopic identification of diatoms was also conducted in order to quantify the number of diatom cells in subsamples collected from the experimental tanks. The subsamples were fixed using borax-buffered formaldehyde at a final concentration of 1% (v/v). After an aliquot (50–100 mL) of the subsample settled in an Utermöhl chamber, the cells were counted under an inverted microscope (NIKON ECLIPSE TE-300, Tokyo, Japan) at a magnification of 200 $\times$ .

## **2.6. High-throughput sequencing**

Water samples (10 mL) were centrifuged at 20,000 *g* for 5 minutes. Genomic DNA (gDNA) was extracted using a modified phenol-chloroform method (Maki et al., 2008). Fragments of 16S rDNA (approximately 500 bp) were amplified from the extracted gDNA by PCR using universal 16S rDNA bacterial primers for the V4 region: 515F (5'- Seq A - TGT GCC AGC MGC CGC GGT AA -3') and 806R (5'- Seq B - GGA CTA CHV GGG TWT CTA AT -3') (Maidak et al., 1997, where Seq A and Seq B represent nucleotide sequences targeted by the second PCR primers. PCR amplification

was performed under the following conditions: denaturation at 94°C for 1 min, annealing at 52°C for 2 min, and extension at 72°C for 2 min for 20 cycles. Fragments of the 16S rDNA PCR products were amplified again using additional PCR forward (5'- Adaptor C – Tag sequence - Seq A -3') and reverse primers (5'- Adaptor D - Seq B -3'), where Adaptors C and D were used for the MiSeq sequencing reaction. The Tag sequence included 8 nucleotides designed for sample identification barcoding. Thermal cycling was performed under the following conditions: denaturation at 94°C for 1 min, annealing at 59°C for 2 min, and extension at 72°C for 2 min for 12 cycles. PCR amplicons from each sample were used for high-throughput sequencing on a MiSeq Genome Sequencer (Illumina, CA, USA). The sequences obtained for each sample were grouped based on tag sequences, and average read lengths of 450 bp were obtained. Negative controls (reactions with no template or template from unused filters) were prepared for all steps of the process after DNA extraction to check for contamination.

Before the analysis of the bacterial community, we removed sequences according to the following criteria: <200 bp in length, with a phred-equivalent quality score of <25, containing ambiguous characters, with an uncorrectable barcode, or missing the primer sequence. The remaining sequences were clustered into phylotypes using QIIME (ver. 1.8.0) with a minimum coverage of 99% and a minimum identity of 97%. The identities of phylotypes were analyzed by comparison of sequences against the DNA Data Bank of Japan (DDBJ) using a BLAST analysis.

## **2.7. Phylogenetic analysis**

Full-length sequences of 16S rDNA (approximately 1,450 bp) were amplified from the extracted gDNA by PCR using the following oligonucleotide primers: 27F, 5'-AGA GTT TGA TCM TGG CTC AG-3'; and 1492R, 5'-GGY TAC CTT GTT ACG ACT T-3' (Maidak et al., 1997). PCR amplicons were cloned using a TA Cloning Kit (Invitrogen, Carlsbad, CA, USA). One hundred clones were obtained for each sample. The amplicons were sequenced using an ABI Dye Deoxy Terminator Cycle Sequencing Kit (Life Technologies, Carlsbad, CA, USA). The 27F primer was used as the sequencing primer. Sequences were assigned to phylotypes using BLAST to identify their closest matching sequences. Select clone sequences related to the dominant phylotypes detected by MiSeq sequencing analysis were chosen for additional sequencing using the 1492R primer. Phylogenetic trees including clone sequences were constructed according to the neighbor-joining algorithm using TreeViewPPC (Saitou and Nei, 1987).

## **2.8. Accession numbers**

The DDBJ accession numbers for the 16S rDNA clone sequences obtained in this study are shown in Table 2. All sequences have been deposited in the DDBJ database (accession number of the submission is PRJDB4118).

## **3. Results**

### **3.1. Changes in chemical compounds and DAPI-stained particles**

Ambient seawater samples had relatively low nitrate concentrations of  $0.16 \pm 0.05$

$\mu\text{mol L}^{-1}$ . The addition of snow solutions containing aerosol particulates initially resulted in an increase in the nitrate concentration to more than  $1.10 \mu\text{mol L}^{-1}$  (ANOVA;  $P < 0.05$ ) (Fig. 2a). The snow samples used in this study harbored higher concentrations of nitrate ( $35.0 \mu\text{eq L}^{-1}$ ) than those in other snow layers (Fig. S1). Thus, the soluble fraction of aerosol particulates likely released nitrate into the seawater. The initial concentration of soluble nitrate was mostly similar in both the HS and LS tanks regardless of aerosol treatment, because nitrate attached to insoluble particulates (eg.; mineral particles) might be slowly released into the seawater. After the incubation, nitrate in the LS and HS treatments decreased slightly to low concentrations of below  $0.5 \mu\text{mol L}^{-1}$ , similar to levels in the C tank. The C tank maintained a low concentration of nitrate during the incubation. In contrast, the initial concentrations of phosphate in the all three sets of tanks (C, LS, and HS) were similar, ranging from  $0.13 \mu\text{mol L}^{-1}$  to  $0.33 \mu\text{mol L}^{-1}$ , and only the HS tank showed a gradual increase of phosphate to  $0.83 \mu\text{mol L}^{-1}$  during the 2-day incubation (ANOVA;  $P < 0.05$ ) (Fig. 2b). The iron concentration increased proportionally to the amount added in the snow solution (ANOVA;  $P < 0.05$ ), and was maintained during the incubation period (Fig. 2c). These results indicate that the snow-solution treatments added nitrate, phosphate, and iron to the LS and HS tanks.

During microscopic observations using DAPI staining, several types of fluorescent particles were observed in the subsamples, mainly composed of bacteria and yellow fluorescent particles. Most bacteria emitting blue fluorescence were observed as a single cell, while some formed heterogeneous aggregates ranging from  $2.0 \mu\text{m}$  to  $50 \mu\text{m}$  in

diameter. Yellow fluorescent particles, thought to be organic matter, ranged from 1.0  $\mu\text{m}$  to 10  $\mu\text{m}$  in diameter. The bacteria in the LS and HS tanks increased from approximately  $5.0 \times 10^4$  cells  $\text{mL}^{-1}$  to  $8.5 \times 10^4$  cells  $\text{mL}^{-1}$  during the 2 days of incubation, while those in the control seawater fluctuated at relatively low concentrations of approximately  $4.0 \times 10^4$  cells  $\text{mL}^{-1}$  (Table 1). The concentration of yellow particles in the LS and HS tanks increased to  $1.18 \times 10^4$  particles  $\text{mL}^{-1}$  and  $0.77 \times 10^4$  particles  $\text{mL}^{-1}$ , respectively, and decreased to  $0.89 \times 10^4$  particles  $\text{mL}^{-1}$  and  $0.34 \times 10^4$  particles  $\text{mL}^{-1}$ , respectively, after 1 day of incubation. In contrast, yellow particles remained under the detection limit in the C tank.

### **3.3. Abundance and composition of phytoplankton**

There was a significant increase in total Chl *a* concentration in the LS and HS tanks from approximately  $0.90 \mu\text{g L}^{-1}$  to more than  $2.40 \mu\text{g L}^{-1}$  during the 2-day incubation, corresponding to the observed decrease in nitrate (ANOVA;  $P < 0.05$ ) (Fig. 3a). In contrast, the total concentration of Chl *a* in the C tank gradually decreased from  $1.1 \mu\text{g L}^{-1}$  to  $0.2 \mu\text{g L}^{-1}$  during the incubation. This suggests that the nitrate from the snow-solution treatments stimulated phytoplankton growth. In particular, Chl *a* from the size fraction  $>20 \mu\text{m}$  in the LS and HS tanks significantly increased (ANOVA;  $P < 0.05$ ) after the incubation (Fig. 3b) compared to the smaller size fractions, indicating that this was primarily due to the growth of large-celled eukaryotic photoautotrophs (Fig. 3c–e).

Observation of the phytoplankton community under a microscope confirmed the growth of Bacillariophyta (diatoms), mainly comprised of *Pseudo-nitzschia* and

*Chaetoceros* species in the LS and HS treatments, respectively (Fig. S5). During the incubation, cell concentrations of *Pseudo-nitzschia* species significantly increased from less than  $0.85 \times 10^5$  cells mL<sup>-1</sup> to  $6.90 \times 10^5$  cells mL<sup>-1</sup> in the LS and HS tanks (ANOVA;  $P < 0.05$ ), while cell concentrations in the C tank fluctuated from  $0.28 \times 10^5$  to  $0.72 \times 10^5$  cells mL<sup>-1</sup> (Fig. 4). In the HS tank, *Chaetoceros* species increased in concentration from  $0.45 \times 10^5$  to  $6.00 \times 10^5$  cells mL<sup>-1</sup> during the incubation period. In contrast, *Chaetoceros* species maintained relatively low densities of less than  $0.35 \times 10^5$  cells mL<sup>-1</sup> in both the C and LS tanks.

#### **3.4. Bacterial community structure**

For the bacterial community analysis, we obtained a total of 447,411 sequences with an average length of 450bp. After sequences were filtered for quality a total of 382,801 remained, with sequence library size for each sample normalized at 27,388. Phylogenetic assignment of sequences revealed that overall the diverse data set was comprised of representatives of 13–18 classes, and 37–47 families (Fig. 5). We found similar patterns among the rarefaction curves determined for the 6 subsamples (Fig. S6a). A UniFrac weighted analysis confirmed bacterial communities from LS and HS tanks were distinct from the untreated control (C) (Fig. S6b).

The majority of phylotypes belonged to 6 classes, namely, the Cyanobacteria, Acidimicrobiia, Flavobacteria, Alpha- and Gamma-proteobacteria, and SAR406, which are typically observed in marine environments (Fig. 5a). The phylotypes belonging to the Cyanobacteria had a low relative abundances ranging from 0.5% to 2.9% (Fig. 5b).

The bacterial composition was similar among all three (C, LS and HS) tanks at day 0, whereas relative abundances of some bacterial groups changed after the incubation in the snow-solution treatments (LS and HS) compared to the control (C). In the class Alpha-proteobacteria, representatives of the family Rhodobacteraceae were relatively high in abundance in the HL and HS tanks (18.7% and 14.8%, representatively), while they only accounted for 7.8% of sequences in the C tank. In the class Gamma-proteobacteria, sequences belonging to the family Colwelliaceae had a relative abundance greater than 9.6% in the HS tank after incubation, whereas those of the C and LS tanks were equal or less than 0.6%. In contrast, the phylotype ratios of the family Halomonadaceae decreased from 19.1% to 10.2%, which corresponded to the increasing amount of snow solution added to the treatments. The phylotypes belonging to the AB16 group in the SAR406 class, known to be pelagic bacteria, decreased from approximately 4.5% to less than 1% in the snow-solution treated seawater after incubation, while their relative abundance in the control tank remained above 3.0%.

### **3.5. Phylogenetic analysis of full-length 16S rDNA sequences**

The 16S rDNA PCR amplicons from the clone libraries produced a total of 172 clones from all three (C, LS, and HS) tanks. The 16S rDNA sequences mainly belonged to the following six classes: Cyanobacteria, Actinobacteria, Bacilli, Bacteroidetes, Alpha- and Gamma-proteobacteria, as well as the chloroplast group, and included 15 families that overlapped with the MiSeq sequencing database (Table 2). We found that 14 representative clones formed clusters with known bacterial sequences belonging to

these families, which dominated the MiSeq sequencing database (Fig. 6). Chloroplast sequences from diatoms, such as *Pseudo-nitzschia seriata* and *Thalassiosira pseudonana*, were often detected from clone libraries recovered from the LS and HS tanks. Most clones belonging to the class Alpha-proteobacteria were closely related to *Roseobacter* species in the family Rhodobacteraceae (DSE12-5-583L-7, DSE12-5-583H-30), and *Pelagibacter* species in the SAR clade (DSE12-5-Control-1, DSE12-5-583L44). In the class Gamma-proteobacteria, the clone DSE12-5-583H-5 belonging to the family *Colwelliaceae* was related to *Colwellia* species. The sequences DSE12-5-Control-14 and DSE12-5-583L-15 classified as Gamma-proteobacteria clustered with pelagic bacteria (*Bacterium* WHC3-1) in the order *Oceanospirillales*. Some sequences of the class *Bacteroidetes* (DSE12-5-583L-31, DSE12-5-Control-31) and the class SAR 406 (Control-33) were detected in all three (C, LS and HS) tanks (Table 2).

## **4. Discussion**

### **4.1. Changes in nutrient and particle concentrations**

Aerosol deposition to oceanic surface waters inputs various compounds including metals, nitrate and sulfate, and is thought to influence primary production, export production, and carbon sequestration (Zhang and Liu, 1994; Erickson et al., 2003; Tan et al., 2011). This is thought to potentially influence primary production, export production, and carbon sequestration although data are scarce. Here we add new insight to this important issue by demonstrating that aerosol dust input results in significant

changes to the surface microbiota. Major changes observed included an increase in diatom biomass and changes in phytoplankton and bacterial diversity, which appeared to be linked to the alleviation of nitrate limitation. Diatom blooms in response to aerosol dust events have also been observed in the western North Pacific (Yuan and Zhang, 2006).

Organic matter associated with dust-mineral particles has been reported to be deposited in coastal areas and stimulate the growth of marine heterotrophic bacteria (Lekunberri et al., 2010). Additionally, dust addition experiments have previously led to a 1.5- to 3-fold increase in bacterial abundance and activity in seawater (Bonnet et al., 2005; Herut et al., 2005; Pulido-Villena et al., 2008). Taken together, these results indicate that nitrate and organic matter associated with aerosol deposition stimulate microbial growth in nutrient-deficient seawater.

Unlike nitrate, concentrations of phosphate and iron in all experimental tanks remained still or changed regardless of the growth patterns of microorganisms. Phosphate concentrations did not change immediately after the addition of snow, but instead gradually increased over the 2 days of incubation (Fig. 2b). Phosphate attached to the aerosols would require additional days of incubation in order to be released into the experimental tanks. In contrast, higher concentrations of iron were measured immediately after the snow solution was added, and these levels were maintained at their initial values throughout the incubation period (Fig. 2c). The deposition of Asian-dust mineral particles has been reported to provide iron to the open ocean. Iron is also a growth-limiting nutrient for oceanic phytoplankton communities (Duce and

Tindale, 1991) in our study, however, iron levels did not appear to be growth limiting.

#### **4.2. Dynamics of phytoplankton composition**

Diatoms belonging to the Bacillariophyta, such as species in the *Pseudo-nitzschia* and *Chaetoceros*, were observed in the snow-solution treated seawater, while members of Chlorophyta were not found in any experimental tanks (Fig. 4). The chloroplast sequences of diatoms were mainly detected in the clone library recovered from the snow-solution treated seawater (Table 2). In the MiSeq sequencing database, the Stramenopiles, including the chloroplasts of diatoms, were relatively higher in abundance in the snow-solution treated seawater than the control (data not shown). Furthermore, these diatoms are categorized as microplankton, which are typically 20–150  $\mu\text{m}$  in size. The Chl *a* concentration in the large size fraction ( $>20 \mu\text{m}$ ) increased in the treated seawater (Fig. 3). Diatoms often increase in the western North Pacific after Asian dust events (Yuan and Zhang, 2006). Consequently, nitrate enrichment caused by the addition of snow solution likely accelerated the growth of Bacillariophyta (in particular *Pseudo-nitzschia* and *Chaetoceros* species).

#### **4.3. Bacterial community dynamics**

We conclude that aerosol dust input causes changes to existing marine bacterial populations rather than acting as a source of inoculum for dust-borne bacteria. Dust aerosols are reported to include terrestrial bacterial species, mainly belonging to the phyla Actinobacteria and Firmicutes (Maki et al., 2011; Tanaka et al., 2011). The

bacterial communities in snow samples used in this experiment were also dominated by these phyla as well as the Beta-proteobacteria, whereas treated tanks harbored communities dominated by marine bacteria (Fig. S7). Shipboard experiments conducted during other voyages in May 2013 also identified an increase in these bacteria due to aerosol supplements (Asahi et al. 2016, Fig. S8).

Sequences from the family Rhodobacteraceae recovered from the clone library were classified into clusters within the genus *Roseobacter* (Fig. 6) and were closely related to the sequences previously recovered from a variety of pelagic marine environments in the North Pacific Ocean and East Sea. *Roseobacter* species in the family Rhodobacteraceae have been associated with phytoplankton blooms (Elifantz et al., 2013), and they grow abundantly under high-nutrient conditions in marine environments (Wagner-Döbler and Biebl, 2006, Yeo et al., 2013). The genus *Roseobacter* includes ubiquitous marine bacteria, which contribute to the metabolization of a large variety of organic compounds and the demethylation of algae-producing DMSP (dimethylsulfoniopropionate) in oceanic environments (Brinkhoff et al., 2008), and are often reported to increase in relative abundance in seawater amended with organic matter (Landa et al. 2013). Members of Colwelliaceae are also known to degrade organic matter, such as aromatic hydrocarbons, which are stable in aquatic environments (Mason et al., 2014). Moreover, the bacterial species belonging to the families Rhodobacteraceae (Wagner-Döbler and Biebl, 2006) and *Colwelliaceae* (Mason et al., 2014) have been reported to consume nitrate via denitrification pathways. Therefore, in the snow solution-treated seawater, increased

nitrate and organic matter leading to more yellow particles and microalgal cells, would induce the growth of heterotrophic bacteria (including representatives from the Colwelliaceae and Rhodobacteraceae), implying consequences for the carbon cycle in these aerosol-affected waters.

In contrast, in the MiSeq sequencing database, phylotypes belonging to the SAR406 clade, Pelagibacteraceae, and Halomonadaceae decreased in seawater treated with snow solution over the course of the 2-day incubation (Fig. 5b). The clones recovered from subsamples collected from the experimental tanks clustered with sequences from members of the SAR406 clade, which are often detected in oligotrophic ocean regions (Table 2, Fig. 6) (Gordon and Giovannoni, 1996; Pham et al., 2008). The *Pelagibacter* representative of the Alpha-proteobacteria belonged mainly to the SAR clade, which dominate in the oligotrophic regions of the Pacific Ocean. Individuals from the family Halomonadaceae are members of the order Oceanospirillales, clones of which were more abundant in the clone libraries recovered from the control compared to the treated seawaters, and were related to pelagic bacterial sequences (Bacterium WBC-3-9) (Martinez-Garcia et al., 2012). Since marine bacterial communities, such as the *Pelagibacter* of the SAR clade, are mainly composed of obligate oligotrophic bacteria (Giovannoni and Stingl, 2005), nutrient enrichment is thought to reduce their growth.

## 5. Conclusions

In conclusion, we demonstrated that snow-borne aerosol particulates from the

Asian continent have a measurable impact on the sea surface microbial community of the Pacific Ocean. Diatom growth was enhanced following the release of nitrate from snow and shifts in the bacterial community also occurred in the oligotrophic seawater after aerosol exposure. In the future, aerosol transport due to Chinese economic and industrial development is expected to increase the long-range transport of aerosols and aerosol deposition. This study highlights the potential impact that changes in aerosol production could have on marine chemistry and microbiology.

### **Acknowledgements**

We are grateful to the captain and crew of the T/S Seisui Maru for their support at sea. Members of Fasmac Co., Ltd. helped with the MiSeq sequencing analyses. This research was supported by a Grant-in-Aid for the Encouragement of Young Scientists (26340049, 26304003) from the Ministry of Education, Culture, Sports, Science, and Technology of Japan. The Bilateral Joint Research Projects from the Japan Society for the Promotion of Science also supported this work, as did the Strategic International Collaborative Research Program (SICORP: 7201006051).

### **References**

Asahi, Y., Maki, T., Ishikawa, A., Mastunaga, T., Watanabe, K., Aoki, K., Horiuchi, A., Hasegawa, H., Iwasaka, Y., 2016. Effects of the snow solution include aerosol

- particles on microbial compositions in the northwest Pacific Ocean. Bull. Soc. Sea Water Sci. Jpn. 70, 28–40. (in Japanese)
- Blank, M., Leinen, M., Prospero, J.M., 1985. Major Asian aeolian inputs indicated by the mineralogy of aerosols and sediments in the western North Pacific. Nature 314, 84–86.
- Bonnet, S., Guieu, C., Chiaverinni, J., Ras, J., Stock, A., 2005. Effect of atmospheric nutrients on the autotrophic communities in a low nutrient, low chlorophyll system. Limnol. Oceanogr. 50, 1810–1819.
- Brinkhoff, T., Giebel, H.A., Simon, M., 2008. Diversity, ecology, and genomics of the *Roseobacter* clade: a short overview. Arch. Microbiol., 189, 531–539.
- Chan, C.K., Yao, X., 2008. Air pollution in mega cities in China. Atmospheric Environment 42: 1–42.
- DiTullio, G.R., Laws, E.A., 1991. Impact of an atmospheric-oceanic disturbance on phytoplankton community dynamics in the North Pacific Central Gyre. Deep Sea Res. I 38, 1305–1329.
- Duce, R.A., Tindale, N.W., 1991. Atmospheric transport of iron and its deposition in the ocean; Chemistry and biology of iron and other trace metals. Limnol. Oceanogr. 36, 1715–1726.
- Erickson III, D.J., Hernandez, J.L., Ginoux, P., Gregg, W.W., McClain, C., Christian, J., 2003. Atmospheric iron delivery and surface ocean biological activity in the Southern Ocean and Patagonian region. Geophysic Res. Lett. 30, 1609–1613.

- Elifantz, H., Horn, G., Ayon, M., Cohen, Y., Minz, D., 2013. *Rhodobacteraceae* are the key members of the microbial community of the initial biofilm formed in Eastern Mediterranean coastal seawater. *FEMS Microbiol. Ecol.* 85, 348–357.
- Giovannoni, S.J., Stingl, U., 2005. Molecular diversity and ecology of microbial plankton. *Nature*, 437, 343–348.
- Gordon, D.A., Giovannoni, S.J., 1996. Detection of stratified microbial populations related to *Chlorobium* and *Fibrobacter* species in the Atlantic and Pacific oceans. *Appl. Environ. Microbiol.* 62, 1171–1177.
- Hashimoto, S., Horimoto, N., Yamaguchi, Y., Ishimaru, T., Saino, T., 2005. Relationship between net and gross primary production in the Sagami Bay, Japan. *Limnol. Oceanogr.* 50, 1830–1835.
- Herut, B., Zohary, T., Krom, M.D., Mantoura, R.F.C., Pitta, P., Psarra, S., Rassoulzadegan, F., Tanaka, T., Thingstad, T.F., 2005. Response of east Mediterranean surface water to Saharan dust: on-board microcosm experiment and field observations. *Deep Sea Res. II* 52, 3024–3040.
- Hervàs, A., Camarero, L., Reche, I., Casamayor, E.O., 2009. Viability and potential for immigration of airborne bacteria from Africa that reach high mountain lakes in Europe. *Environ. Microbiol.* 11, 1612–1623.
- Jo, C.O., Lee, J.Y., Park, K.A., Kim, Y.H., Kim, K.R., 2007. Asian dust initiated early spring bloom in the northern East/Japan Sea. *Geophysical Res. Lett.* 34, L05602.

- Jordi, A., Basterretxea, G., Tovar-Sánchez, A., Alastuey, A., Querol, X., 2012. Copper aerosols inhibit phytoplankton growth in the Mediterranean Sea. *Proc. National Academy Sci.* 109, 21246–21249.
- Landa, M., Cottrell, M.T., Kirchman, D.L., Blain, S., Obernosterer, I., 2013. Changes in bacterial diversity in response to dissolved organic matter supply in a continuous culture experiment. *Aquat. Microb. Ecol.* 69, 157–168.
- Lekunberri, I., Lefort, T., Romero, E., Vázquez-Domínguez, E., Romera-Castillo, C., Marrasé, C., Peters, F., Weinbauer, M., Gasol, J.M., 2010. Effects of a dust deposition event on coastal marine microbial abundance and activity, bacterial community structure and ecosystem function. *J. Plankton Res.* 32, 381–396.
- Maidak, B. L., Olsen, G. J., Larsen, N., Overbeek, R., McCaughey, M. J., Woese, C., 1997. The RDP (ribosomal database project). *Nucleic Acids Res.* 25, 109–110.
- Maki, T., Aoki, K., Kobayashi, F., Kakikawa, M., Tobo, Y., Matsuki, A., Hasegawa, H., Iwasaka, Y., 2011. Characterization of halotolerant and oligotrophic bacterial communities in Asian desert dust (KOSA) bioaerosol accumulated in layers of snow on Mount Tateyama, Central Japan, *Aerobiologia* 27. 277–290.
- Maki T., Susuki S., Kobayashi F., Kakikawa M., Yamada M., Higashi T., Chen B., Shi G., Hong C., Tobo Y., Hasegawa H., Ueda K., and Iwasaka Y., Phylogenetic diversity and vertical distribution of a halobacterial community in the atmosphere of an Asian dust (KOSA) source region, Dunhuang City, *Air Qual. Atmos. Health* 1, 2008, 81–89.
- Martinez-Garcia, M., Brazel, D. M., Swan, B. K., Arnosti, C., Chain, P. S., Reitenga, K.

- G., Xie, G., Poulton, N. J., Gomez, M. L., Masland, D. E., Thompson, B., Bellows, W. K., Ziervogel, K., Lo, C. C., Ahmed, S., Gleasner, C. D., Detter, C. J., Stepanauskas, R., 2012. Capturing single cell genomes of active polysaccharide degraders: an unexpected contribution of *Verrucomicrobia*. *PLoS One* 7. e35314.
- Mason, O.U., Han, J., Woyke, T., Jansson, J.K., 2014. Single-cell genomics reveals features of a *Colwellia* species that was dominant during the Deepwater Horizon oil spill. *Front. Microbiol.* 5.
- Mostajir, B., Dolan, J.R., Rassoulzadegan, F., 1995. A simple method for the quantification of a class of labile marine pico-and nano-sized detritus: DAPI Yellow Particles (DYP). *Aqua. Microbial. Ecol.* 9, 259–266.
- Osada, K., Iida, H., Kido, M., Matsunaga, K., Iwasaka, Y., 2004. Mineral dust layers in snow at Mount Tateyama, Central Japan: formation processes and characteristics. *Tellus* 56B, 382–392.
- Parsons, T.R., Maita, Y., Lalli, C.M., 1984. A manual of chemical and biological methods for seawater analysis. Pergamon, Oxford.
- Paytan, A., Mackey, K.R.M., Chen, Y., Lima, I.D., Doney, S.C., Mahowald, N., Labiosa, R., Post, A.F., 2009. Toxicity of atmospheric aerosols on marine phytoplankton. *Proc. National Academy Sci.* 106, 4601–4605.
- Pham, V.D., Konstantinidis, K.T., Palden, T., DeLong, E.F., 2008. Phylogenetic analyses of ribosomal DNA - containing bacterioplankton genome fragments from a 4000 m vertical profile in the North Pacific Subtropical Gyre. *Environ. Microbiol.* 10, 2313–2330.

- Prospero, J.M., Savoie, D.L., 1989. Effect of continental sources on nitrate concentrations over the Pacific Ocean. *Nature* 339, 687 – 689.
- Pulido-Villena, E., Wagener, T., Guieu, C., 2008. Bacterial response to dust pulses in the western Mediterranean: implications for carbon cycling in the oligotrophic ocean. *Global Biogeochemical Cycles* 22, doi:10.1029/2007GB003091.
- Romero, E., Peters, F., Marrasé, C., Guadayol, Ò., Gasol, J. M., Weinbauer, M. G., 2011. Coastal Mediterranean plankton stimulation dynamics through a dust storm event: An experimental simulation. *Estuarine Coastal Shelf Sci.* 93, 27–39.
- Russell, W.C., Newman, C., Williamson, D.H., 1974. A simple cytochemical technique for demonstration of DNA in cells infected with mycoplasmas and viruses. *Nature* 253, 461–462.
- Spokes, L.J., Jickells, T.D., 1996. Factors controlling the solubility of aerosol trace metals in the atmosphere and on mixing into seawater. *Aquat. Geochem.* 1, 355–374.
- Saitou, N., Nei, M., 1987. The neighbor-joining method: A new method for reconstructing phylogenetic trees. *Mol. Biol. Evol.* 4, 406–425.
- Strickland, J.D.H., Parsons, T.R., 1972. A practical hand-book of seawater analysis. *Fish. Res. Bd. Can. Bull.* 167, 1–311.
- Suzuki, R., Ishimaru, T., 1990. An improved method for the determination of phytoplankton chlorophyll using N, N- dimethyl- formamide. *J. Oceanogr. Soc. Jpn.* 46, 190–194.
- Suzuki K., Tsunogai S., 1993. Origin of calcium in aerosol over the western north

- Pacific. J. Atmos. Chem. 6, 363–374.
- Tan, S.C., Shi, G.Y., Shi, J.H., Gao, H.W., Yao, X., 2011. Correlation of Asian dust with chlorophyll and primary productivity in the coastal seas of China during the period from 1998 to 2008. J. Geophys. Res. 116, G02029.
- Tan, S.C., Yao, X., Gao, H.W., Shi, G.Y., Yue, X., 2013. Variability in the Correlation between Asian Dust Storms and Chlorophyll a Concentration from the North to Equatorial Pacific. PLoS ONE 8, e57656.
- Tanaka, D., Tokuyama, Y., Terada, Y., Kunimochi, K., Mizumaki, C., Tamura, S., Wakabayashi, M., Aoki, K., Shimada, W., Tanaka, H., Nakamura, S., 2011. Bacterial communities in Asian dust-containing snow layers on Mt. Tateyama, Japan. Bull. Glaciological. Res. 29, 31–39.
- Uematsu M., Duce R.A. and Prospero J.M., Deposition of atmospheric mineral particles in the North Pacific Ocean, J. Atmos. Chem. 3, 1985, 123–138.
- Wagner-Döbler, I., Biebl, H., 2006. Environmental biology of the marine *Roseobacter* lineage. Annu. Rev. Microbiol. 60, 255–280.
- Watanabe, K., Saito, Y., Tamura, S., Sakai, Y., Eda, N., Aoki, M., Kawabuchi, M., Yamada, H., Iwai, A., Kawada, K., 2011. Chemical characteristics of the snow pits at Murododaira, Mount Tateyama, Japan. Ann. Glaciol. 52, 102–110.
- Yeo, S.K., Huggett, M.J., Eiler, A., Rappe, M.S., 2013. Coastal bacterioplankton community dynamics in response to a natural disturbance. PLoS ONE 8, E56207.
- Yuan, W., Zhang, J., 2006. High correlations between Asian dust events and biological productivity in the western North Pacific. Geophysical Res. Lett. 33, L07603.

Zhang, J., Liu, M. G., 1994. Observations on nutrient elements and sulphate in atmospheric wet depositions over the northwest Pacific coastal oceans-Yellow Sea. *Mar. Chem.* 47, 173–189.

## Figure legends

Fig. 1. Snow samples were collected from Murododaira (36.58°N, 137.60°E) on Mt. Tateyama. The shipboard incubation experiment was performed in the Pacific Ocean at Site A (34.07°N, 138.77°E).

Fig. 2. Changes in the concentration of nitrate, phosphate, and iron in the control (C), light dust event (LS), and high dust event (HS) tanks. Seawater samples were collected at Site A in the Pacific Ocean on 26 May 2012 and incubated for 2 days. The error bars were calculated from samples obtained from one 20-L and two 4-L experimental tanks.

Fig. 3. Change in chlorophyll concentrations in the unfiltered subsample and the subsample fractions of >20  $\mu\text{m}$ , 10–20  $\mu\text{m}$ , 2.0–10  $\mu\text{m}$ , and <2.0  $\mu\text{m}$  in the control (C), light dust event (LS), and high dust event (HS) tanks. Seawater samples were collected at Site A in the Pacific Ocean on 26 May 2012 and incubated for 2 days.

Fig. 4. Concentrations of cells classified as *Pseudo-nitzschia* and *Chaetoceros* species, and other diatom species in the control (C), light dust event (LS), and high dust event (HS) 20-L experimental tanks, at time points 0, 1, and 2 days.

Fig. 5. Bacterial composition at the (a) class and (b) family level of the partial sequences in the MiSeq sequencing database (approximately 400 bp) obtained from the

control (C), light dust event (LS), and high dust event (HS) 20-L experimental tanks, at initial and 2-day time-points.

Fig. 6. Phylogenetic tree constructed from the partial sequences of 16S rDNA amplicons obtained from the clone libraries from the control (C), light dust event (LS), and high dust event (HS) tanks, and the known members of Cyanobacteria, Flavobacteria, Alpha-proteobacteria and Gamma-proteobacteria. The phylogenetic tree was calculated from a dissimilarity matrix of an approximately 550 bp alignment (*E. coli* numbered from 41 to 592) using a neighbor-joining algorithm. The names of representative clones (DSE12-5 series) are indicated. Open circles at branch points indicate bootstrap values obtained by the neighbor-joining analysis exceeded 50% after 1,000 replicate samplings.

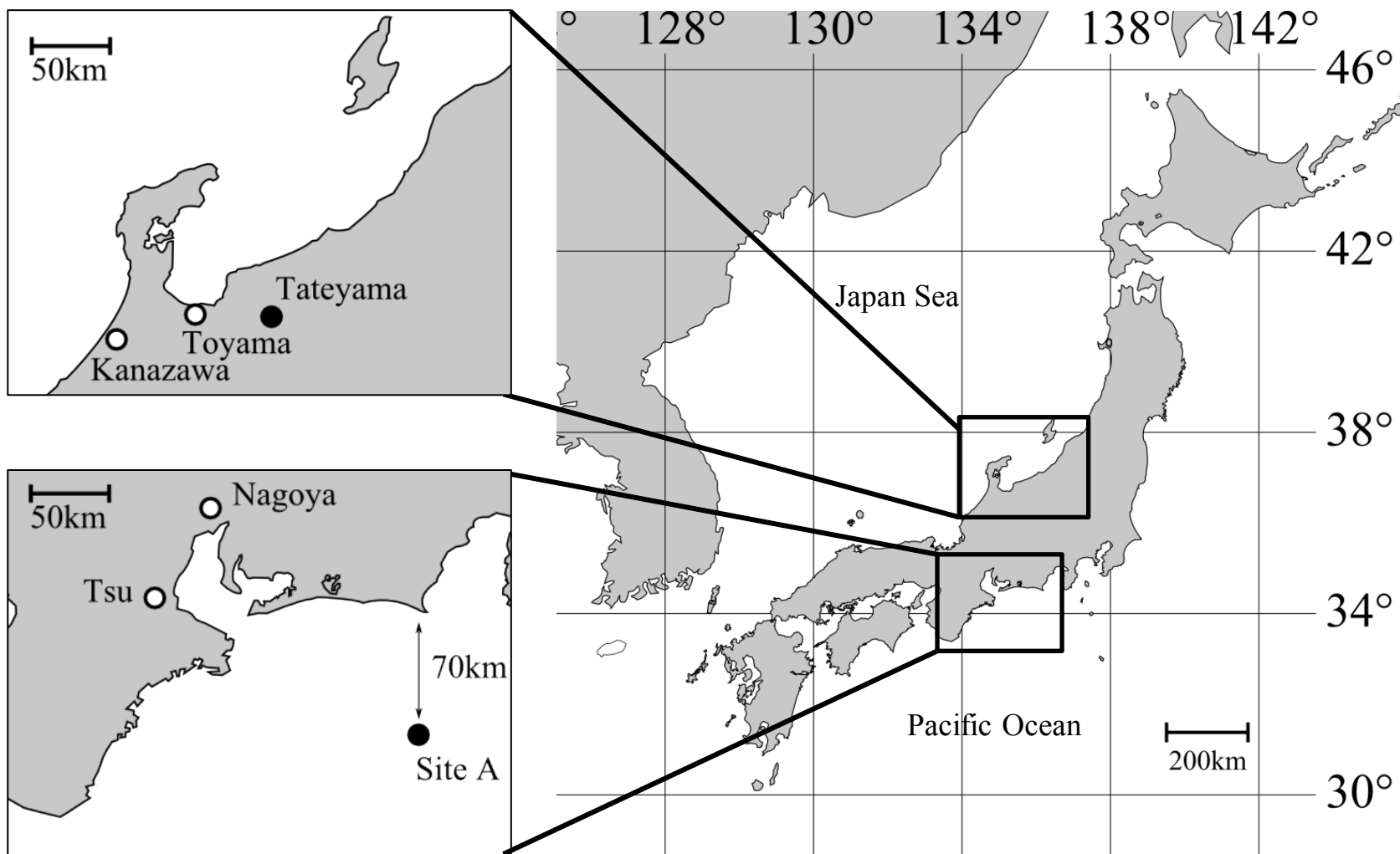


Fig. 1 T. Maki et al.

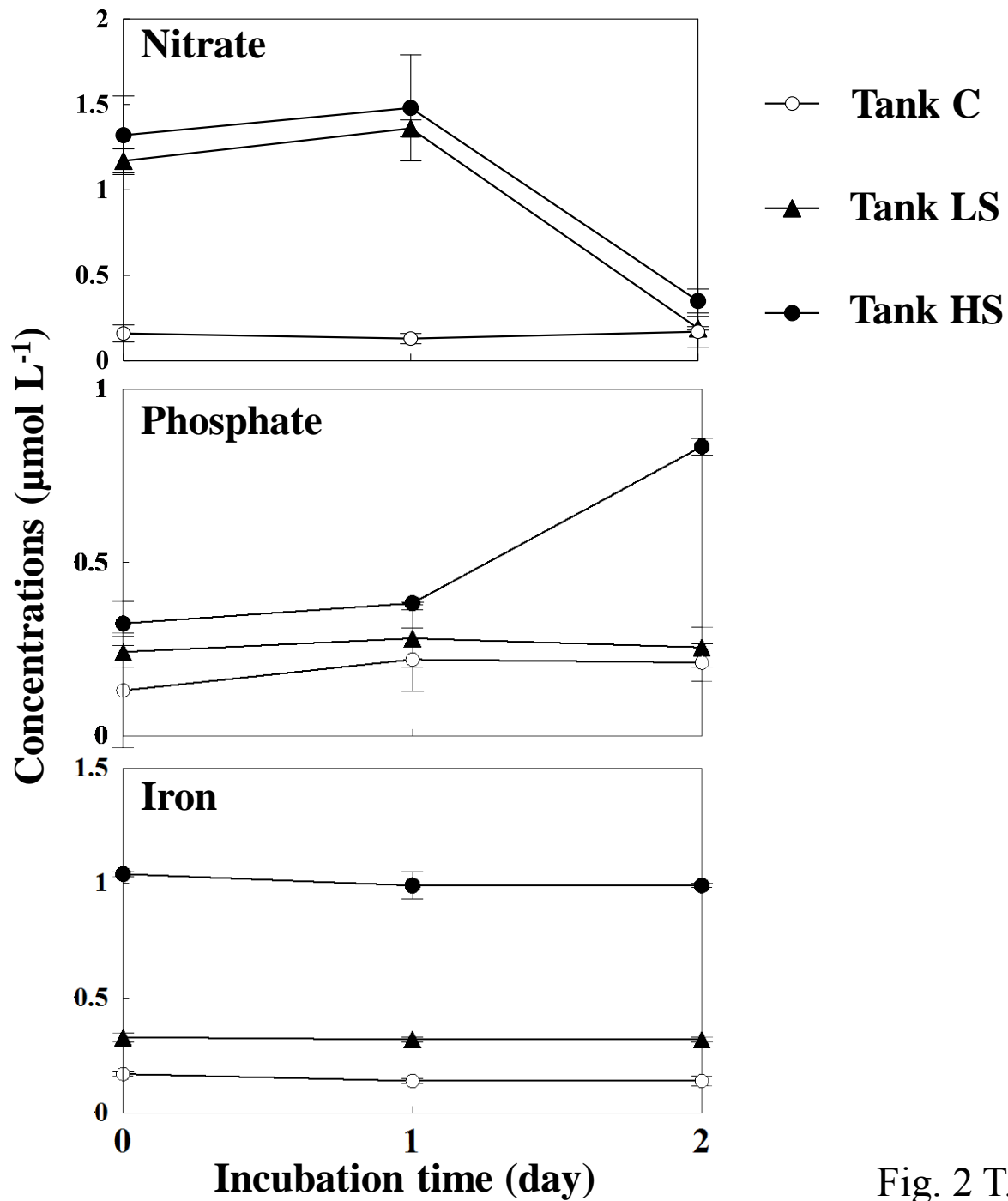


Fig. 2 T. Maki et al.

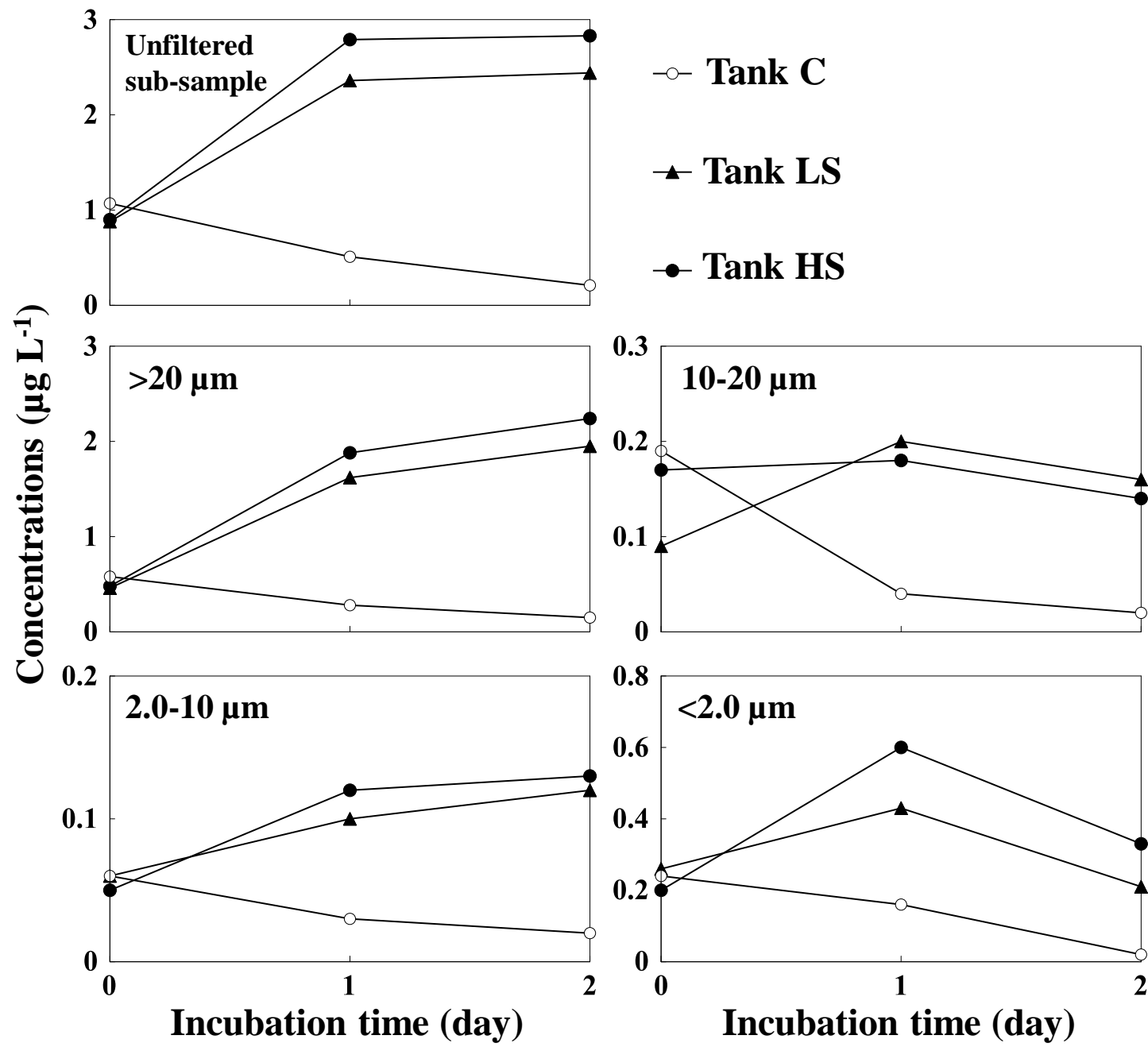


Fig. 3 T. Maki et al.

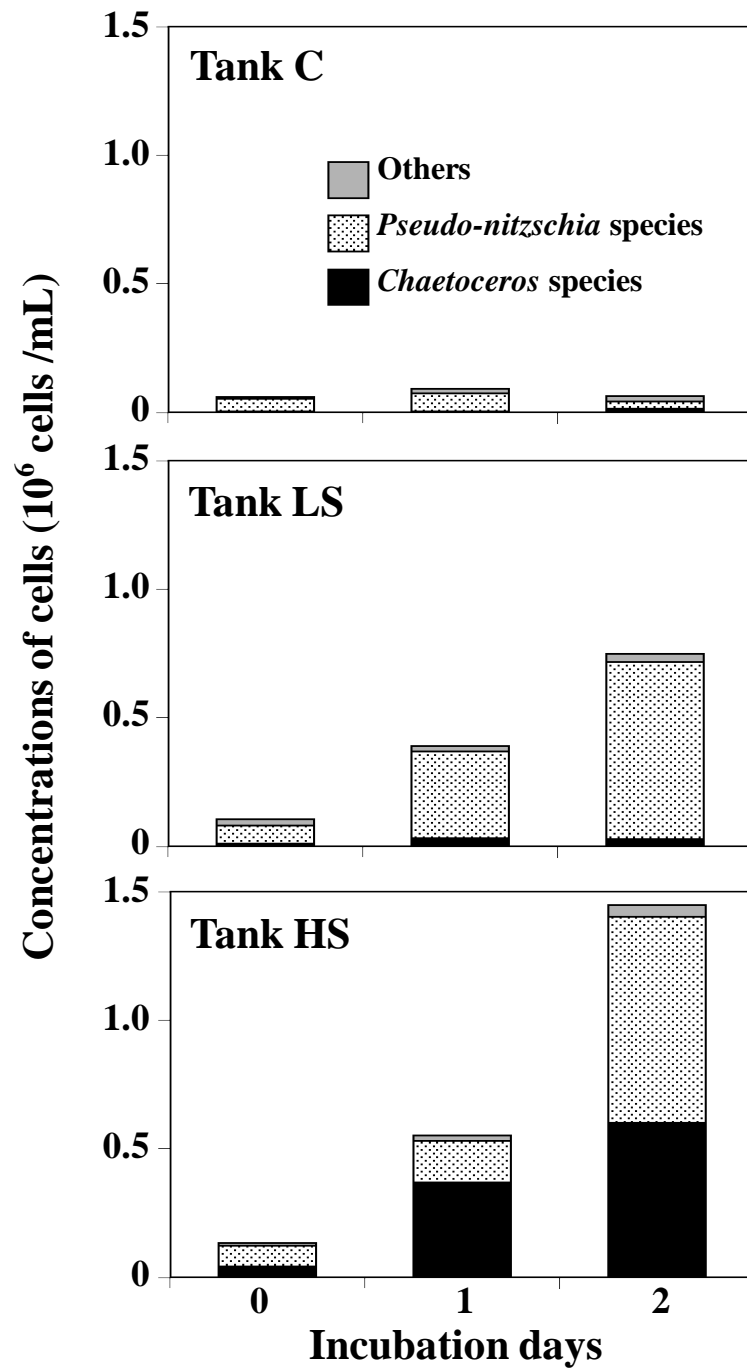
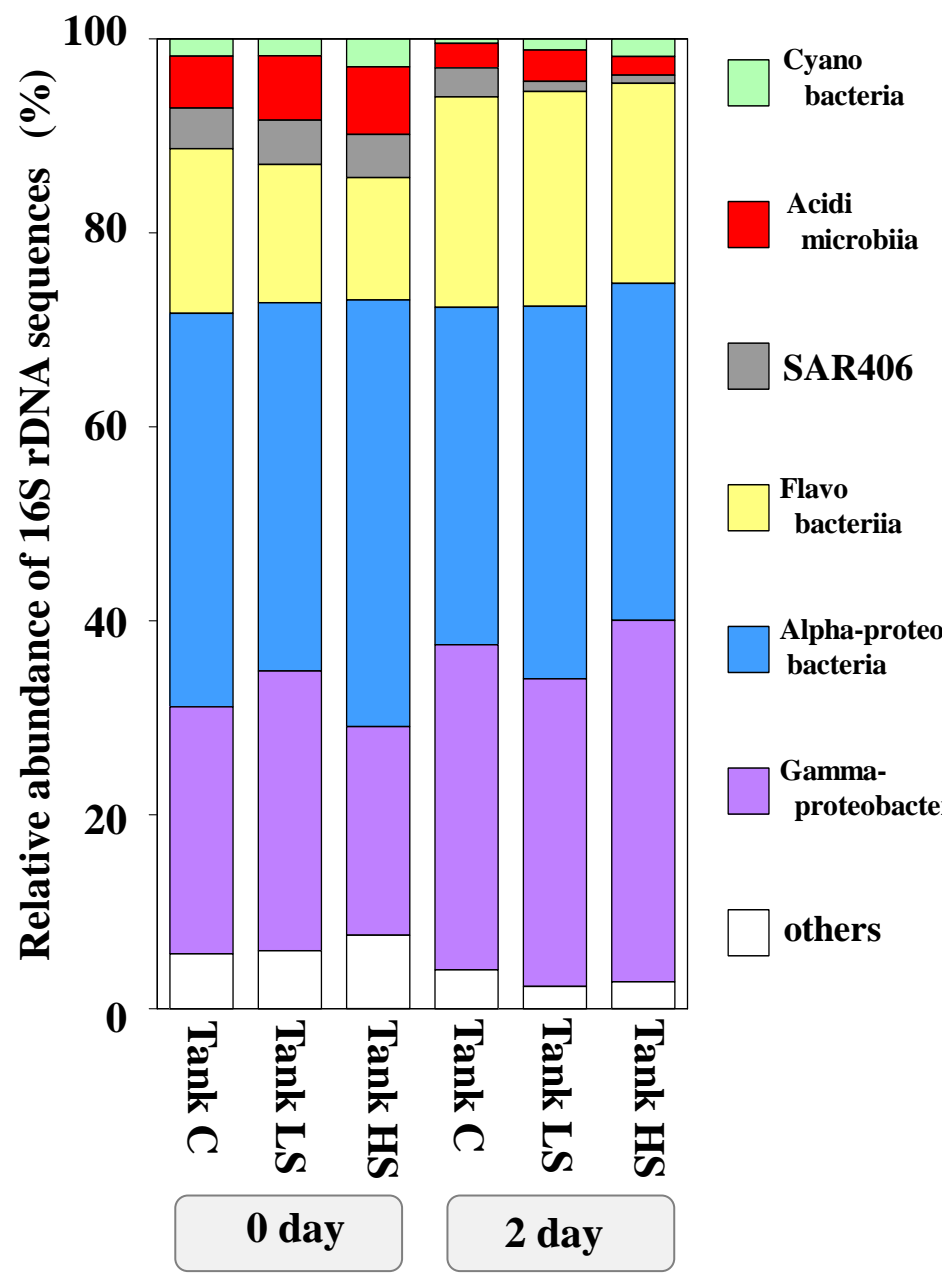


Fig. 4 T. Maki et al.

**Class level**



**Family level**

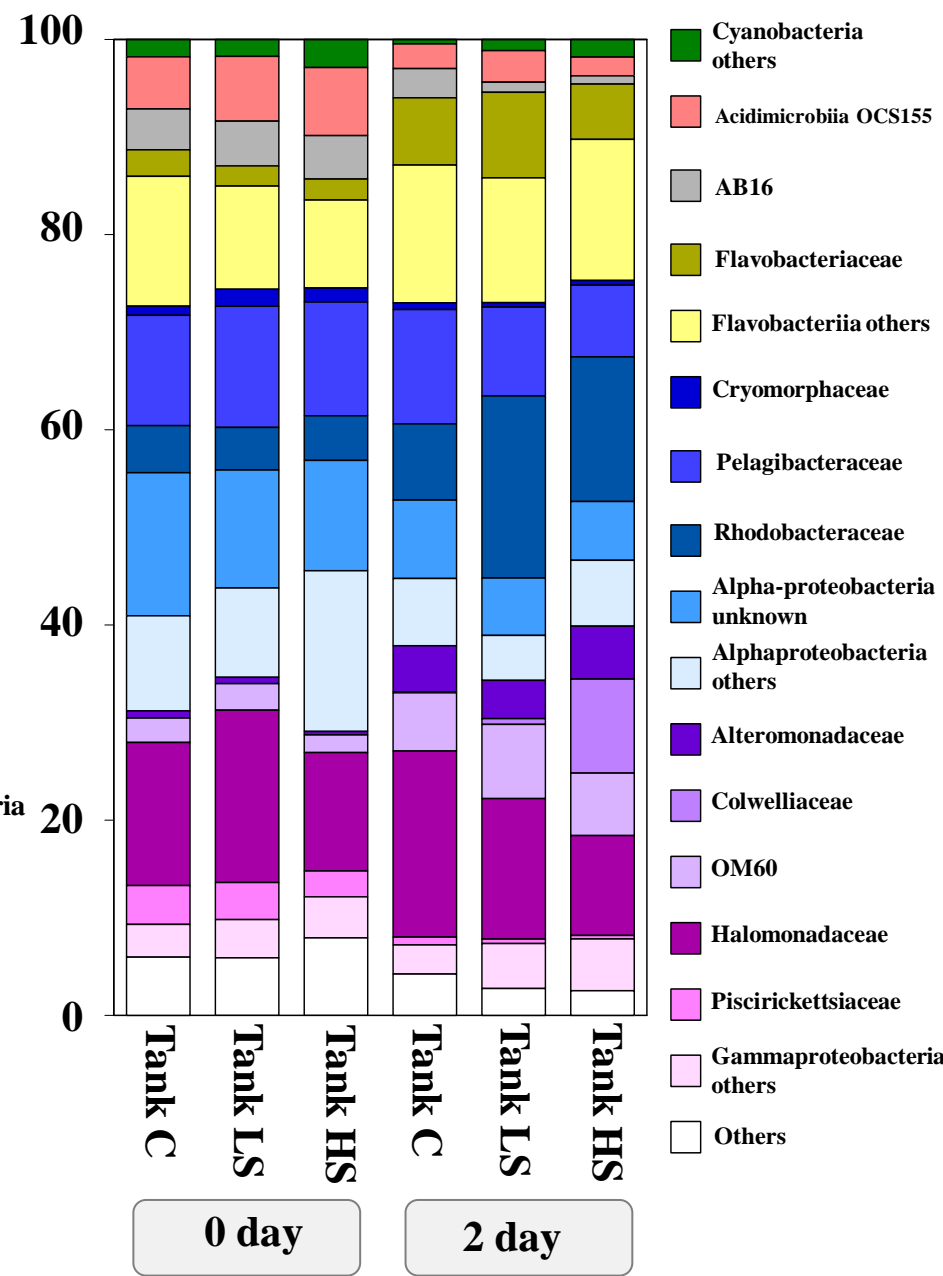


Fig. 5 Maki et al.

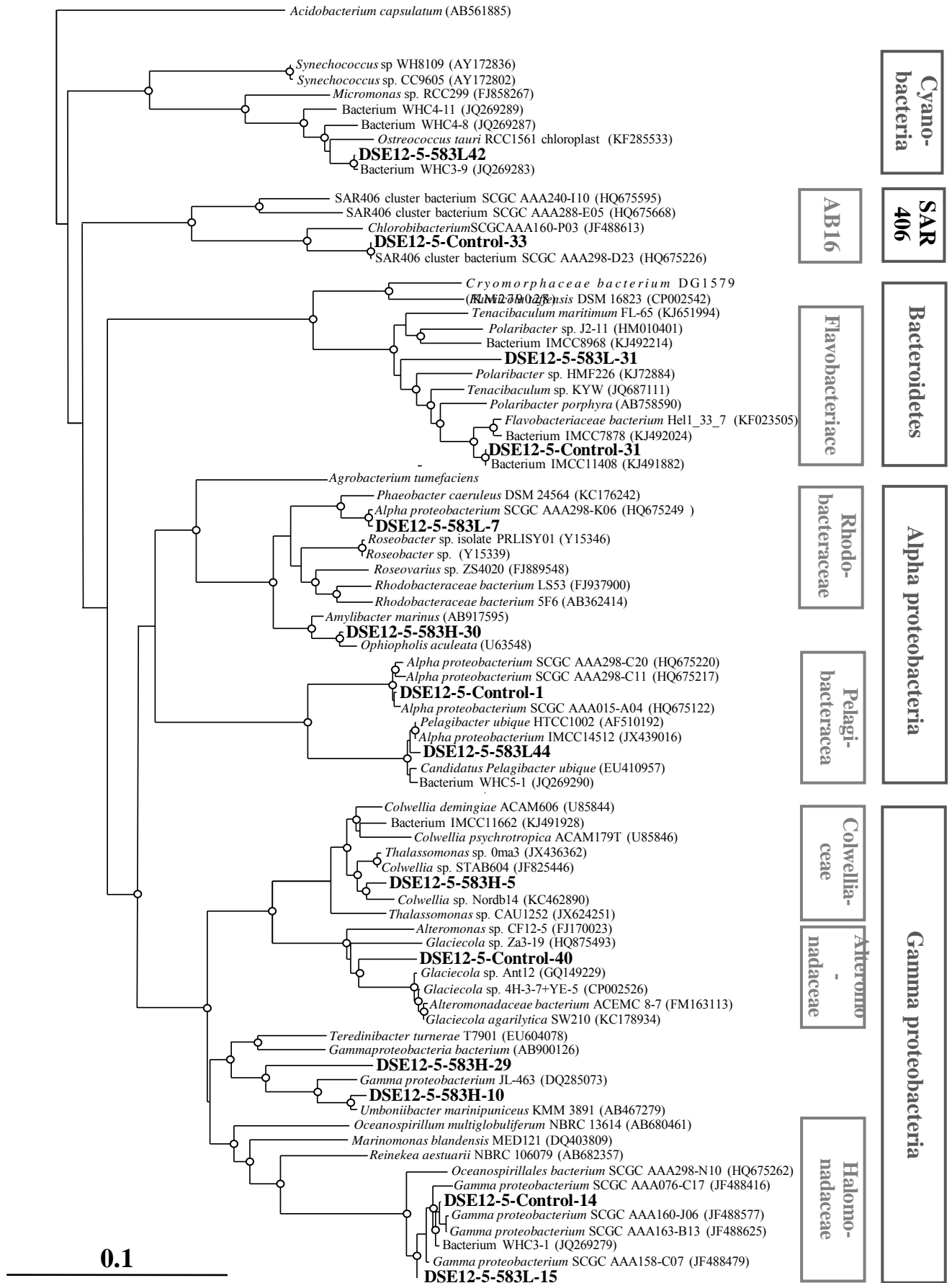


Fig. 6 T. Maki et al.

**Table 1. Concentration of DAPI fluorescent particles in the control (C), light dust event (LS), and high dust event (HS) tanks.**

Incubation time (day)	Bacterial particles *			Yellow fluorescence particles *		
	C	LS	HS	C	LS	HS
0	4.16 ± 1.43	5.70 ± 1.62	4.83 ± 1.07	< 0.1	0.77 ± 0.39	1.18 ± 0.27
1	3.69 ± 0.87	5.85 ± 0.92	5.31 ± 1.69	< 0.1	0.34 ± 0.14	0.89 ± 0.43
2	3.95 ± 1.08	8.53 ± 4.00	8.76 ± 2.11	< 0.1	0.22 ± 0.19	0.86 ± 0.57

\* Standard deviation was obtained from the values in one 20 L and two 4 L experimental tanks.

(10<sup>5</sup> particles mL<sup>-1</sup>)

**Table 2. Phylogenetic affiliation of 16S rDNA gene sequences obtained from clone libraries.**

Category	Numbers of clones <sup>*1</sup>			Representative clone name <sup>*2</sup>	Length (bp) <sup>*3</sup>	GenBank accession no.	Closest relative	Similarity (%) <sup>*4</sup>
	Control	1 mL snow solution	5 mL snow solution					
Cyanobacteria	0	4	2	DSE12-5-583L-42	590	LC088185	Bacterium WHC3-9 (JQ269283)	587/590(99.5%)
Actinobacteria	0	1	1	DSE12-5-583L-11	587	LC088186	<i>Phytomonospora</i> sp. KT1403 (KJ755850)	509/590 (86.3%)
	0	2	0	DSE12-5-583L-38	519	LC088187	Actinobacterium SCGC AAA163-G08 (JF488172)	511/520 (98.3%)
	0	1	0	DSE12-5-583L-26	522	LC088188	<i>Kribbella catacumbae</i> (KM096442)	461/522 (88.3%)
Alpha-proteobacteria	10	10	9	DSE12-5-583L-44	591	LC088189	Candidatus <i>Pelagibacter ubique</i> HTCC1062 (CP000084)	586/591 (99.2%)
	5	4	2	DSE12-5-Control-1	536	LC088190	Alpha proteobacterium SCGC AAA298-C11 (HQ675217)	532/536 (99.3%)
	4	2	1	DSE12-5-Control-3	641	LC088191	Alpha proteobacterium HIMB5 (CP003809)	633/641 (98.8%)
	1	1	0	DSE12-5-Control-41	752	LC088192	Candidatus <i>Pelagibacter ubique</i> (EU410957)	696/752 (92.6%)
	0	3	0	DSE12-5-583L-7	646	LC088193	alpha proteobacterium SCGC AAA160-J18 (JF488581)	638/646 (98.8%)
	1	3	4	DSE12-5-583H-30	571	LC088194	Bacterium IMCC4848 (KJ491760)	571/571 (100%)
	Bacteroidetes	1	2	2	DSE12-5-Control-31	564	LC088195	Bacterium IMCC11498 (KJ491882)
1		1	1	DSE12-5-583H-24	592	LC088196	Bacterium WHC3-2 (JQ269280)	566/592 (95.6%)
1		1	0	DSE12-5-583L-31	582	LC088197	<i>Polaribacter</i> sp. HMF2268 (KJ728849)	538/582 (92.4%)
Gamma-proteobacteria	14	5	5	DSE12-5-Control-14	720	LC088198	Bacterium WHC3-1 (JQ269279)	716/720 (99.4%)
	1	1	1	DSE12-5-583L-15	590	LC088199	Bacterium WHC3-1 (JQ269279)	587/590 (99.5%)
	1	1	0	DSE12-5-Control-40	706	LC088200	Alteromonadaceae bacterium GWS-BW-H8gM (AY515434)	671/706 (95.0%)
	0	0	2	DSE12-5-583H-29	571	LC088201	Bacterium IMCC8835 (KJ492170)	563/571 (98.6%)
	0	0	1	DSE12-5-583H-5	683	LC088202	<i>Colwellia</i> sp. STAB604 (JF825446)	668/683 (97.8%)
	0	0	1	DSE12-5-583H-12	778	LC088203	Alteromonadaceae bacterium NB0076-02 (KP770091)	767/778 (98.6%)
	0	0	1	DSE12-5-583H-10	791	LC088204	<i>Umboniibacter marinipuniceus</i> (AB467279)	783/791 (99.0%)
Eukaryota	1	1	1	DSE12-5-Control-36	789	LC088205	<i>Pinus merkusii</i> chloroplast (KP771703)	787/789 (99.7%)
	0	2	2	DSE12-5-583L-28	333	LC088206	<i>Thalassiosira pseudonana</i> mitochondrion (DQ186202)	312/337 (92.6%)
	0	1	3	DSE12-5-583L-43	593	LC088207	<i>Pseudo-nitzschia multiseriis</i> chloroplast (KR709240)	583/593 (98.3%)
	0	0	2	DSE12-5-583H-3	619	LC088208	<i>Pseudo-nitzschia multiseriis</i> mitochondrion (KR149143)	582/620 (93.9%)
	0	0	2	DSE12-5-583H-27	592	LC088209	<i>Chaetoceros</i> sp. C134 chloroplast (FJ002204)	586/590 (99.3%)
	0	0	1	DSE12-5-583H-35	775	LC088210	<i>Emiliania huxleyi</i> strain CCMP 373 chloroplast (AY741371)	773/775 (99.7%)
SAR406 (AB16)	1	2	0	DSE12-5-Control-33	563	LC088211	SAR406 cluster bacterium SCGC AAA298-D23 (HQ675226)	563/563 (100%)

\*1 Numbers of the clones in 16S rDNA clone libraries recovered from the seawater samples treated without snow solution, with 1 mL and 5 mL snow solutions.

\*2 Representative clones in 16S rDNA library indicate phylotypes that were classified with more than 97% similarity, and were named as the DSE12-5 series.

\*3 The sequence length of each representative clone.

\*4 Similarity value between each representative clone and the closest relative in databases.